

Micromechanical String Resonators: Analytical Tool for Thermal Characterization of Polymers

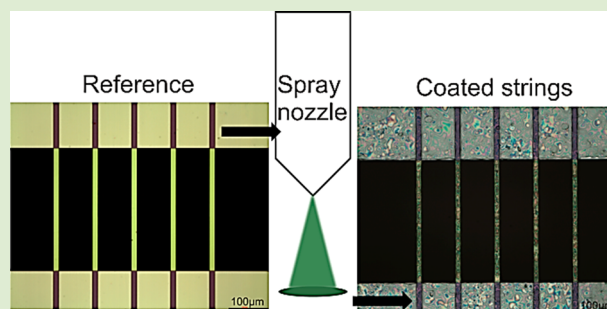
Sanjukta Bose,^{*,†} Silvan Schmid,[†] Tom Larsen,[†] Stephan S. Keller,[†] Peter Sommer-Larsen,[‡] Anja Boisen,[†] and Kristoffer Almdal[†]

[†]Department of Micro- and Nanotechnology, Technical University of Denmark, DTU Nanotech, DK-2800 Kongens Lyngby, Denmark

[‡]Department of Energy Conversion and Storage, Technical University of Denmark, DTU Energy Conversion, DK-4000 Roskilde, Denmark

S Supporting Information

ABSTRACT: Resonant microstrings show promise as a new analytical tool for thermal characterization of polymers with only few nanograms of sample. The detection of the glass transition temperature (T_g) of an amorphous poly(D,L-lactide) (PDLLA) and a semicrystalline poly(L-lactide) (PLLA) is investigated. The polymers are spray coated on one side of the resonating microstrings. The resonance frequency and quality factor (Q) are measured simultaneously as a function of temperature. Change in the resonance frequency reflects a change in static tensile stress, which yields information about the Young's modulus of the polymer, and a change in Q reflects the change in damping of the polymer-coated string. The frequency response of the microstring is validated with an analytical model. From the frequency independent tensile stress change, static T_g values of 40.6 and 57.6 °C were measured for PDLLA and PLLA, respectively. The frequency-dependent damping from Q indicates higher T_g values of 62.6 and 88.8 °C for PDLLA and PLLA, respectively, at $\sim 10^5$ Hz. Resonant microstrings facilitate thermal analysis of nanogram polymer samples measuring the static and a dynamic glass transition temperature simultaneously.



Polymer thin films are widely used in microtechnology¹ and biomedical applications² where the knowledge of the exact polymer properties is crucial. Micro- and nanoscale beam resonators have been utilized as highly sensitive sensors for mass,³ chemicals,⁴ humidity,⁵ or temperature.^{6–8} It has been shown that atomic force microscopy (AFM) can be used in noncontact mode to measure thermal transitions of polymer in micrometer scale.⁹ Another approach is based on microcantilevers (singly clamped beams) that have been used efficiently in detecting phase transitions^{10,11} and loss modulus of polymers.¹² For detecting glass to rubber transition of polymers, the top surface of a cantilever is coated with a thin film of the polymer. The phase transitions of the polymer can then be detected from the temperature dependent deflection and change in resonance frequency. Microcantilevers coated with polymers often show a large initial deflection due to stress generated during deposition, which impedes the optical readout of the mechanical motion.

In this work we use microstrings (doubly clamped beams with tensile prestress). Strings are clamped on both sides and problems with initial out-of-plane deflection are thus avoided. Microstrings enable the characterization of polymer thin films deposited by arbitrary techniques, such as spray coating, inkjet printing, plasma polymerization, and so on.

The glass transition temperature is an important characteristic temperature of polymers. It is the temperature at which the first long-range segmental motions in the polymer chains occur. The Young's modulus of the material is drastically reduced when the temperature is raised above T_g . Common techniques used to determine T_g are differential scanning calorimetry (DSC), dilatometry, dynamic mechanical analysis (DMA), or dielectric spectroscopy (DES). Here we propose to use microstring resonators for thermal characterization of thin polymer films with a total mass of only a few nanograms. With highly sensitive microstrings, we reduce the material required for a measurement by 6 orders of magnitude compared to DSC. The working principle is demonstrated by first spray coating biodegradable amorphous polymer poly(D,L-lactide) (PDLLA) or semicrystalline poly(L-lactide) (PLLA) on silicon nitride (SiN_x) microstrings. We then monitor the resonance frequency and quality factor of the strings while ramping the temperature up. Temperature-induced changes in both parameters can be correlated to the static and dynamic T_g of the polymers.

The static stress in the microstrings is high, ~ 190 MPa, and it is a common valid assumption that the deflection-induced

Received: September 10, 2013

Accepted: December 12, 2013

Published: December 24, 2013

change in tensile stress during vibration is negligible.¹³ Thus, the resonance frequency change is a measure of the heating-related static stress change. Hence T_g detected via the resonance frequency corresponds to the static T_g , which is comparable with T_g detected by DSC. Quality factor (Q), on the other hand, is directly related to the viscoelastic material damping, which is frequency-dependent. Thus, T_g measured via Q corresponds to the dynamic T_g , which is comparable with T_g detected by DES at the corresponding frequency.

First we derive a model describing the temperature-induced frequency detuning of a polymer-coated microstring. The total tensile stress σ_s in a simple string as a function of temperature T is given by⁶

$$\sigma_s = \sigma_0 + (\alpha_F - \alpha_S)E(T - T_0) \quad (1)$$

with initial tensile prestress, σ_0 , thermal expansion coefficient of the frame and string, α_F and α_S , respectively, Young's modulus of the string, E , and temperature T_0 at which σ_0 is defined. The bimaterial string consists of a SiN_x layer with a thickness h_S and a polymer layer with an effective thickness h_P . In this case, an effective stress σ^* can be defined as

$$\begin{aligned} \sigma^* &= \frac{h_S \sigma_S + h_P \sigma_P}{h_S + h_P} \\ &= \{h_S[\sigma_{0,S} + (\alpha_F - \alpha_S)E_S](T - T_0) \\ &\quad + h_P[\sigma_{0,P} + (\alpha_F - \alpha_P)E_P](T - T_0)\} \\ &\quad / (h_S + h_P) \end{aligned} \quad (2)$$

where the parameters with the subscript S and P belong to the SiN_x and polymer, respectively. The eigenfrequency of the bimaterial string is now given by^{6,7}

$$f_0 = \frac{n}{2L} \sqrt{\frac{\sigma^*}{\rho^*}}, \quad n = 1, 2, 3, \dots \quad (3)$$

where n is the resonant mode number, L is the length of the string, and ρ^* is the effective mass density of the string

$$\rho^* = \frac{h_S \rho_S + h_P \rho_P}{h_S + h_P} \quad (4)$$

The eigenfrequency of the string finally becomes

$$f_0 = \frac{n}{2L} \sqrt{\frac{(h_S[\sigma_{0,S} + (\alpha_F - \alpha_S)E_S] + h_P[\sigma_{0,P} + (\alpha_F - \alpha_P)E_P])(T - T_0)}{h_S \rho_S + h_P \rho_P}} \quad (5)$$

If there is no polymer coating present, eq 5 reduces to

$$f_0 = \frac{n}{2L} \sqrt{\frac{\sigma_{0,S} + (\alpha_F - \alpha_S)E_S(T - T_0)}{\rho_S}} \quad (6)$$

which has been derived and applied in the study reported by Larsen et al.⁷ In the case of a high- Q microstring resonator ($Q > 1000$), the eigenfrequency and resonance frequency can be assumed to be equal.

Figures 1 and 2 show the microstring-based thermal analysis of PDLLA and PLLA, respectively, together with respective blank references. The analysis consists of the resonance frequency and Q measured as a function of temperature.

From eq 6 it can be seen that the frequency of a blank SiN_x microstring ($\alpha_S = 1.25$ ppm/K)⁶ on a Si substrate ($\alpha_F = 2.6$ ppm/K) increases with temperature. This behavior is observed for both reference strings (dotted lines in Figures 1a and 2a).

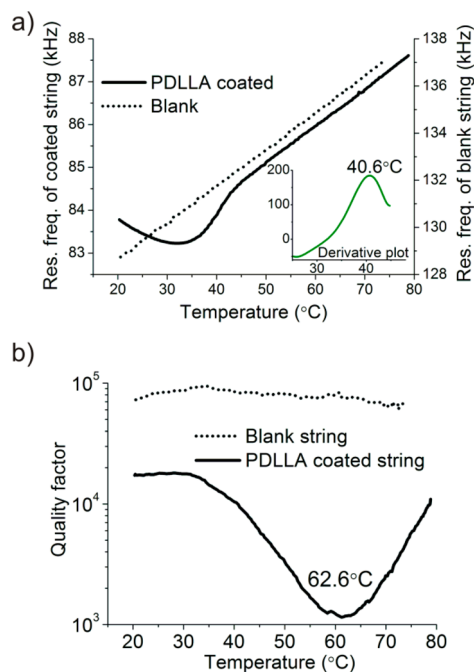


Figure 1. Thermal analysis of PDLLA coated on a 985 μm long, 6 μm wide, and 340 nm thick SiN_x microstring. (a) Resonance frequency change reflecting static stress change; the inset shows the derivative plot indicating the T_g at the peak. (b) Q change as a function of temperature for blank and PDLLA coated strings.

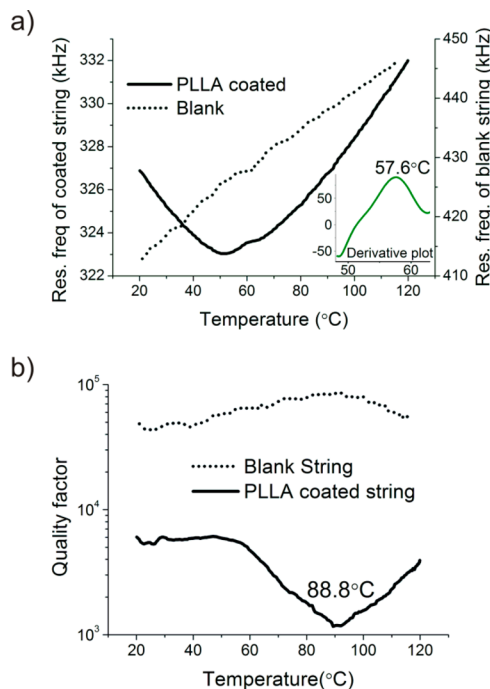


Figure 2. Thermal analysis of PLLA coated on a 316 μm long, 14 μm wide, and 340 nm thick SiN_x microstring. (a) Resonance frequency change reflecting static stress change; the inset shows the derivative plot indicating the T_g at the peak. (b) Q change as a function of temperature for blank and PLLA coated strings.

The frame material is expanding more than the string material with increasing temperature. As a consequence of this the tensile stress in the string increases which results in a higher resonance frequency. When a polymer-coated string is heated,

the frequency initially drops (solid lines in Figures 1a and 2a) due to the larger thermal expansion of the polymer (α_p) with respect to the frame (α_F) and string (α_S). After crossing T_g due to a drastic drop of the Young's modulus of the polymer during the glass–rubber phase transition,¹⁴ the mechanical properties of the string are dominated by the silicon nitride. Above T_g the numerator in the model of a polymer-coated microstring (eq 5) approaches the numerator in the model for a blank string (eq 6). Hence, after the transition, the resonance frequency increases as a function of temperature as it was observed for the blank strings. The Young's modulus of the SiN_x is considered as 250 GPa for the analytical model. Below T_g the Young's modulus of the polymer is assumed to be 3.5 GPa, and above T_g the modulus is assumed to drop 3 orders of magnitude^{14,15} to 3.5 MPa. It can be concluded that the maximal change in the slope of the resonance frequency curve thus corresponds to the maximal change in Young's modulus of the polymer. From the frequency slope maximum (inset of Figures 1a and 2a), T_g of PDLLA and PLLA is then determined to be 40.6 and 57.6 °C, respectively. This corresponds well with T_g of 42.7 and 59.9 °C measured by DSC. These experiments were repeated at least three times to confirm the reported results.

In Figure 3 the analytical model (eq 5) is fitted to the experimental data, with α_p , $\sigma_{0,p}$ and h_p as fitting parameters (see

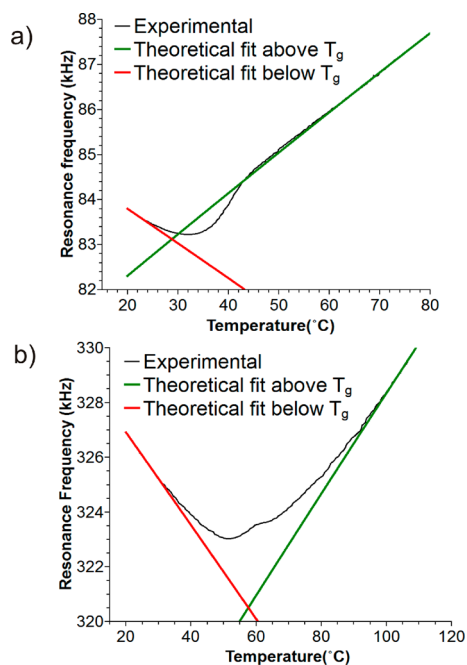


Figure 3. Experimental data and analytical model plotted as a function of temperature for (a) PDLLA and (b) PLLA coated string.

Table 1). The curves below T_g (red line) differ from the fits above T_g (green line) due to a reduced modulus E_p and the tensile prestress in the polymer, $\sigma_{0,p}$. A tensile prestress in the string $\sigma_{0,S}$ of 186 and 197 MPa for PDLLA and PLLA, respectively, was determined before coating at $T_0 = 20$ °C. α_p values obtained from Table 1 are in accordance with the literature values.¹⁶ From the polymer layer thicknesses, a total PDLLA and PLLA mass of 5.9 ng and 6.3 ng, respectively, can be estimated, assuming a mass density of 1248 kg/m³ taken from the polymer data sheet. A thickness of 1.0 μm was measured by white light interferometry for PDLLA deposition

Table 1. Fitting Parameters Obtained from Fitting Eq 5 to Experimental Data (see Figure 3) Measured at $T_0 = 20$ °C

	PDLLA	PLLA
α_p [ppm/K] ($T < T_g$)	80.6	58.4
$\sigma_{0,p}$ [MPa] ($T < T_g$)	-12.4	31.4
α_p [ppm/K] ($T > T_g$)	360.1	299.9
$\sigma_{0,p}$ [MPa] ($T > T_g$)	-14.8	24.1
h_p [μm]	0.78	1.14

on strings. This corresponds well with the effective thickness of ~ 0.8 μm extracted from the analytical model.

In a relaxed mechanical resonator, the quality factor (Q) due to intrinsic material damping is equal to the inverse loss tangent.¹⁰ In an unrelaxed resonator such as a string, the tensile stress leads to an enhancement of Q . This results in that Q becoming a linear function of the loss tangent.¹⁷

$$Q \propto (\tan \delta)^{-1} \quad (7)$$

Thus, T_g of the polymer can be detected at the minimum of the Q versus temperature curve. From Figures 1b and 2b, the frequency dependent glass transitions of PDLLA and PLLA are detected at 62.6 and 88.8 °C, respectively (Figures 1b and 2b, solid line).

As a comparison, the quality factor of the blank reference (Figures 1b and 2b, dotted line) remains unchanged with temperature. Without the dissipative polymer coating, the blank string have significantly higher Q values. Q reaches its minimum at the glass–rubber transition of the polymer where the ratio between the stored elastic energy and that converted to heat during deformation is lowest. Unlike T_g obtained from the resonance frequency (Figures 1a and 2a), T_g determined by means of Q is frequency-dependent. T_g is a kinetic parameter and it is dependent on the mechanical frequency, well-known by the time–temperature superposition where time and temperature can be mathematically interchanged at certain conditions.¹⁸ At a higher frequency, higher temperature is required for a polymer to achieve the equivalent mechanical state that is obtained at a lower frequency. Consequently, the transition shifts to a higher temperature. Since we are performing measurements at a frequency of $\sim 10^5$ Hz, the observed values for T_g are in well agreement with T_g of PDLLA and PLLA at 59.1 and 80.5 °C, respectively, measured from the loss tangent peak at 10^5 Hz obtained from dielectric spectroscopy.

In summary, T_g determination of polymer performed by micro string resonators is a new analytical tool. We estimated an error of ± 2 °C for the static and dynamic T_g . This error mainly comes from the uncertainty in the actual temperature of the microstrings. The microstrings facilitate measurements on reduced sample size (5–6 ng) by 6 orders of magnitude compared to 5–10 mg in DSC. Furthermore, the small thermal masses reduce the time to thermal equilibrium significantly making microstrings a fast and highly sensitive tool for measuring phase transitions of polymer samples.

EXPERIMENTAL SECTION

SiN_x microstrings were fabricated from low-stress, silicon-rich silicon nitride by standard microfabrication.³ 0.5 wt % of PDLLA (ester terminated, M_w 16000 g/mol, Sigma Aldrich) solution was prepared with cyclohexanone as solvent and PLLA (M_w 204800 g/mol, NatureWorks PLA polymer 2003D) with dichloromethane as solvent. Both solvents were procured from Sigma Aldrich and used as received.

The polymer solution was sprayed on the strings with an Exacta Coat Ultrasonic Spraying System¹⁹ (Sonotek, U.S.A.). In all our measurements, the coating uniformity has been found to have an insignificant influence on the measurement results.

The resonance frequency was measured with a laser-Doppler vibrometer (MSA-500 from Polytec GmbH) in high vacuum at a pressure below 3×10^{-5} mbar. The quality factor was determined from the -3 dB bandwidth of the resonance curve. A schematic of the experimental setup is shown in Figure 4. The silicon chip comprising

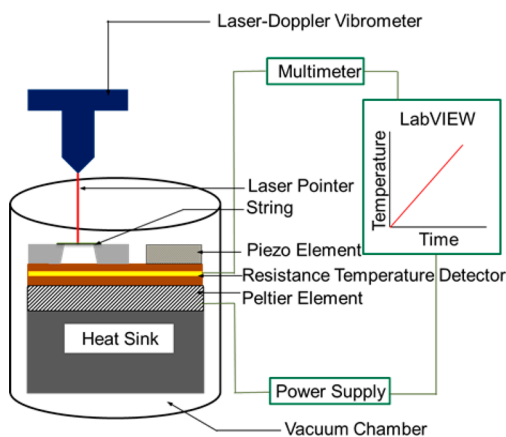


Figure 4. Schematic representation of the experimental set up.

the microstrings was placed on a copper block attached to a Peltier element used for heating and cooling. A resistance temperature detector (RTD; PT-1000) was embedded inside the copper block for measuring the temperature, which was controlled by a LabVIEW based PID controller. Finite Element Method (FEM) simulations (Comsol 4.2) were conducted to investigate the difference in measured temperature and the actual temperature on the strings due to heat loss to the surroundings through radiation in high vacuum. All the temperatures reported are corrected accordingly. For the FEM simulations, thermal conductivities^{20,21} of Si, SiN_x, and the polymers were considered to be 130, 3.2, and 0.175 W/(m K), respectively. Emissivities²² of 0.01, 0.95, and 0.7 were assumed for Si, SiN_x, and polymers, respectively. The strings were actuated with an external piezo element on the copper block. Temperature was varied from 20 to 80 °C for PDLLA and 20 to 120 °C for PLLA at a heating rate of 15 °C/min. Prior to the each measurement, the polymer coated strings were subjected to repeated heating–cooling cycles in order to remove the thermal history.

DSC reference measurements were performed with a DSC Q1000 from TA Instruments. The sample was subjected to heat–cool–heat cycles from 0 to 200 °C at a heating and cooling rate of 10 °C/min. Temperature-dependent measurements of the complex dielectric function were carried out using a Novocontrol Broadband Dielectric Spectrometer BDS-40. The sample cell consisted of two electrodes, the top electrode was 20 mm and the bottom electrode 30 mm in diameter, and the sample was ~ 50 μm thick. The temperature was changed from -100 to 100 °C at a heating rate of 2 °C/min, controlled by a Novocontrol Quattro Cryosystem.

■ ASSOCIATED CONTENT

📄 Supporting Information

The optical microscope images of polymer deposition on the microstrings, the calculated relation between and eigenfrequency and resonance frequency of the microstrings, the differential scanning calorimetry curves and the dielectric loss tangent curves of the polymers used in this study, and the estimation of errors in glass transition temperature detection. This material is available free of charge via the Internet at <http://pubs.acs.org>.

■ AUTHOR INFORMATION

Corresponding Author

*E-mail: sbos@nanotech.dtu.dk.

Notes

The authors declare no competing financial interest.

■ ACKNOWLEDGMENTS

This research is supported by the Villum Kann Rasmussen Centre of Excellence “NAMEC” under Contract No. 65286.

■ REFERENCES

- (1) Lochon, F.; Fadel, L.; Dufour, I.; Rebière, D.; Pistré, J. *Mater. Sci. Eng., C* **2006**, *26*, 348–353.
- (2) Vendra, V. K.; Wu, L.; Krishnan, S. In *Nanostructured Thin Films and Surfaces*; Kumar, C. S. S. R., Ed.; Wiley-VCH: Weinheim, 2010; Vol. 5, pp 1–51.
- (3) Schmid, S.; Dohn, S.; Boisen, A. *Sensors* **2010**, *10*, 8092–8100.
- (4) Lang, H. P.; Baller, M. K.; Berger, R.; Gerber, C.; Gimzewski, J. K.; Battiston, F. M.; Fornaro, P.; Ramseyer, J. P.; Meyer, E.; Güntherodt, H. J. *Anal. Chim. Acta* **1999**, *393*, 59–65.
- (5) Schmid, S.; Kühne, S.; Hierold, C. *J. Micromech. Microeng.* **2009**, *19*, 065018.
- (6) Larsen, T.; Schmid, S.; Grönberg, L.; Niskanen, A. O.; Hassel, J.; Dohn, S.; Boisen, A. *Appl. Phys. Lett.* **2011**, *98*, 121901.
- (7) Larsen, T.; Schmid, S.; Boisen, A. *AIP Conf. Proc.* **2013**, *1552*, 931–936.
- (8) Larsen, T.; Schmid, S.; Villanueva, L.; Boisen, A. *ACS Nano* **2013**, *7*, 6188–6193.
- (9) Meincken, M.; Graef, S.; Sanderson, R. D. *Appl. Phys. A: Mater. Sci. Process.* **2002**, *375*, 371–375.
- (10) Jung, N.; Jeon, S. *Macromolecules* **2008**, *41*, 9819–9822.
- (11) Jung, N.; Seo, H.; Lee, D.; Ryu, C. Y.; Jeon, S. *Macromolecules* **2008**, *41*, 6873–6875.
- (12) Ayala, C.; Heinrich, S. M.; Josse, F.; Dufour, I. *J. Microelectromech. Syst.* **2011**, *20*, 788–790.
- (13) Magnuss, K.; Popp, K. *Schwingungen*; Teubner: Stuttgart, 2005.
- (14) Sperling, L. H. *Introduction to Physical Polymer Science*; John Wiley & Sons, Inc.: Hoboken, NJ, 2005.
- (15) Henton, D.; Gruber, P.; Lunt, J.; Randall, J. *Nat. Fibers, Biopolym., Biocompos.* **2005**, 527–578.
- (16) Meng, Q. K.; Hetzer, M.; De Kee, D. J. *Compos. Mater.* **2010**, *45*, 1145–1158.
- (17) Schmid, S.; Jensen, K.; Nielsen, K.; Boisen, A. *Phys. Rev. B* **2011**, *84*, 1–6.
- (18) Chartoff, R. P.; Menczel, J. D.; Dillman, S. H. *Thermal Analysis of Polymer Fundamental and Applications*; John Wiley & Sons, Inc.: Hoboken, NJ, 2009; pp 387–495.
- (19) Bose, S.; Keller, S. S.; Alstrøm, T. S.; Boisen, A.; Almdal, K. *Langmuir* **2013**, *29*, 6911–6919.
- (20) Sultan, R.; Avery, A. D.; Stiehl, G.; Zink, B. L. *J. Appl. Phys.* **2009**, *105*, 043501.
- (21) Kim, H.-S.; Chae, Y. S.; Park, B. H.; Yoon, J.-S.; Kang, M.; Jin, H.-J. *Curr. Appl. Phys.* **2008**, *8*, 803–806.
- (22) Ravindra, N. M.; Abedrabbo, S.; Tong, F. M.; Nanda, A. K.; Speranza, A. C. *IEEE Trans. Semicond. Manuf.* **1998**, *11*, 30–39.